



Journal of Geophysical Research Solid Earth

Supporting information for

Sustained water loss in California's mountain ranges  
during severe drought from 2012 through 2015 inferred from GPS

Donald F. Argus<sup>1</sup>, Felix W. Landerer<sup>1</sup>, David N. Wiese<sup>1</sup>, Hilary R. Martens<sup>2</sup>,  
Yuning Fu<sup>3</sup>, James S. Famiglietti<sup>1</sup>, Brian F. Thomas<sup>4</sup>, Thomas G. Farr<sup>1</sup>,  
Angelyn W. Moore<sup>1</sup>, Michael M. Watkins<sup>1</sup>

<sup>1</sup>NASA Jet Propulsion Laboratory, California Institute of Technology, Pasadena, USA

<sup>2</sup>Department of Geosciences, University of Montana, Missoula, USA

<sup>3</sup>School of Earth, Environment, and Society, Bowling Green State University, Ohio, USA

<sup>4</sup>Department of Geology and Environmental Science, University of Pittsburgh, Pennsylvania, USA

This supporting information consists of  
Figures S1 to S20

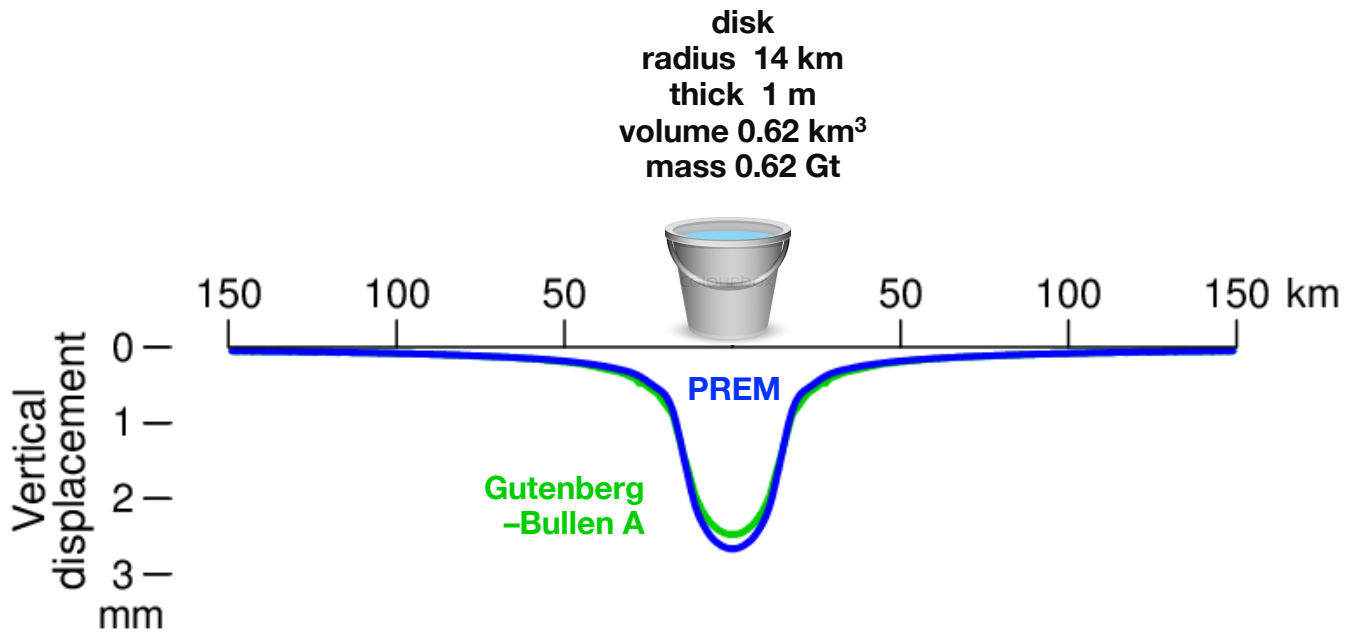


**Fig. S1.** Solid Earth's elastic response to a mass load. Vertical displacement produced by loading of a disk of water 1 m thick and 14 km in radius calculating using Green's functions for (blue) the (PREM) Preliminary Reference Earth Model [Wang et al. 2012, Dziewonski and Anderson 1981] and for (green) the Gutenberg-Bullen A Earth model [Farrell 1972].

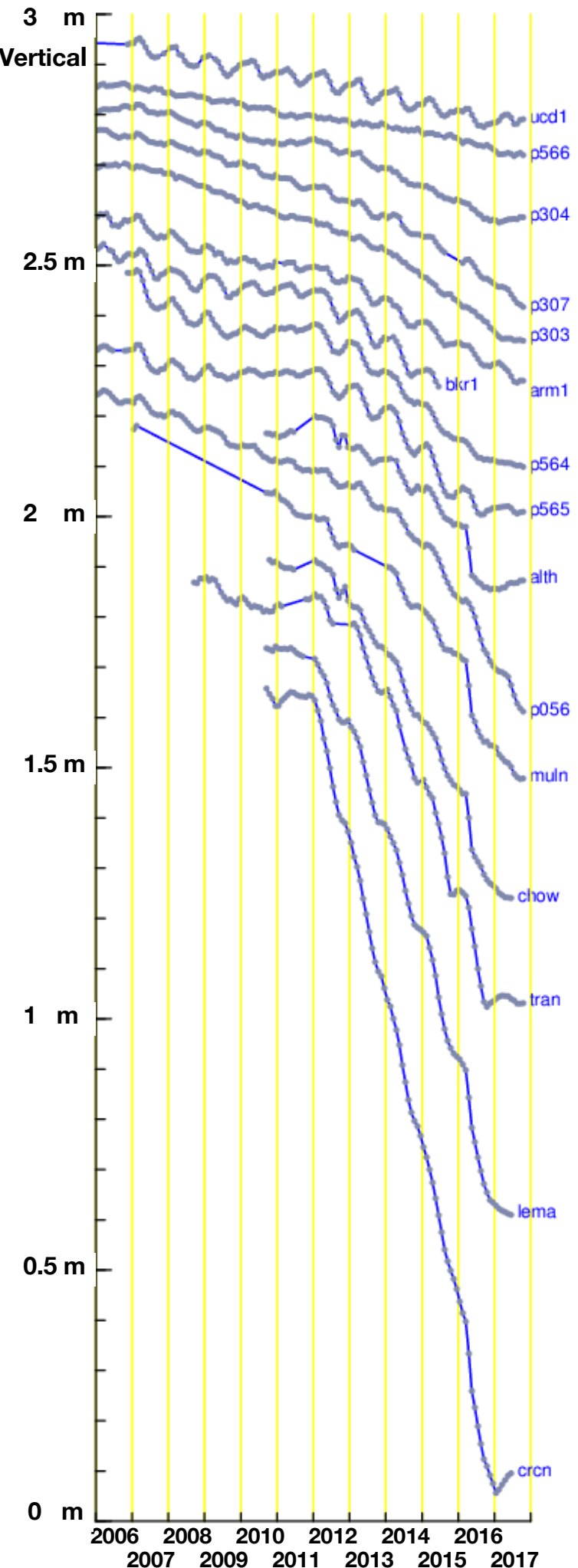


**Fig. S2.** GPS sites in Central Valley subsiding faster than 10 mm/yr. Vertical displacement of 16 GPS sites in porous response to groundwater loss. The rate of subsidence quickened in 2012 at bkr1, p564, p565, alth, p056, chow, tran, lema, and crcn.

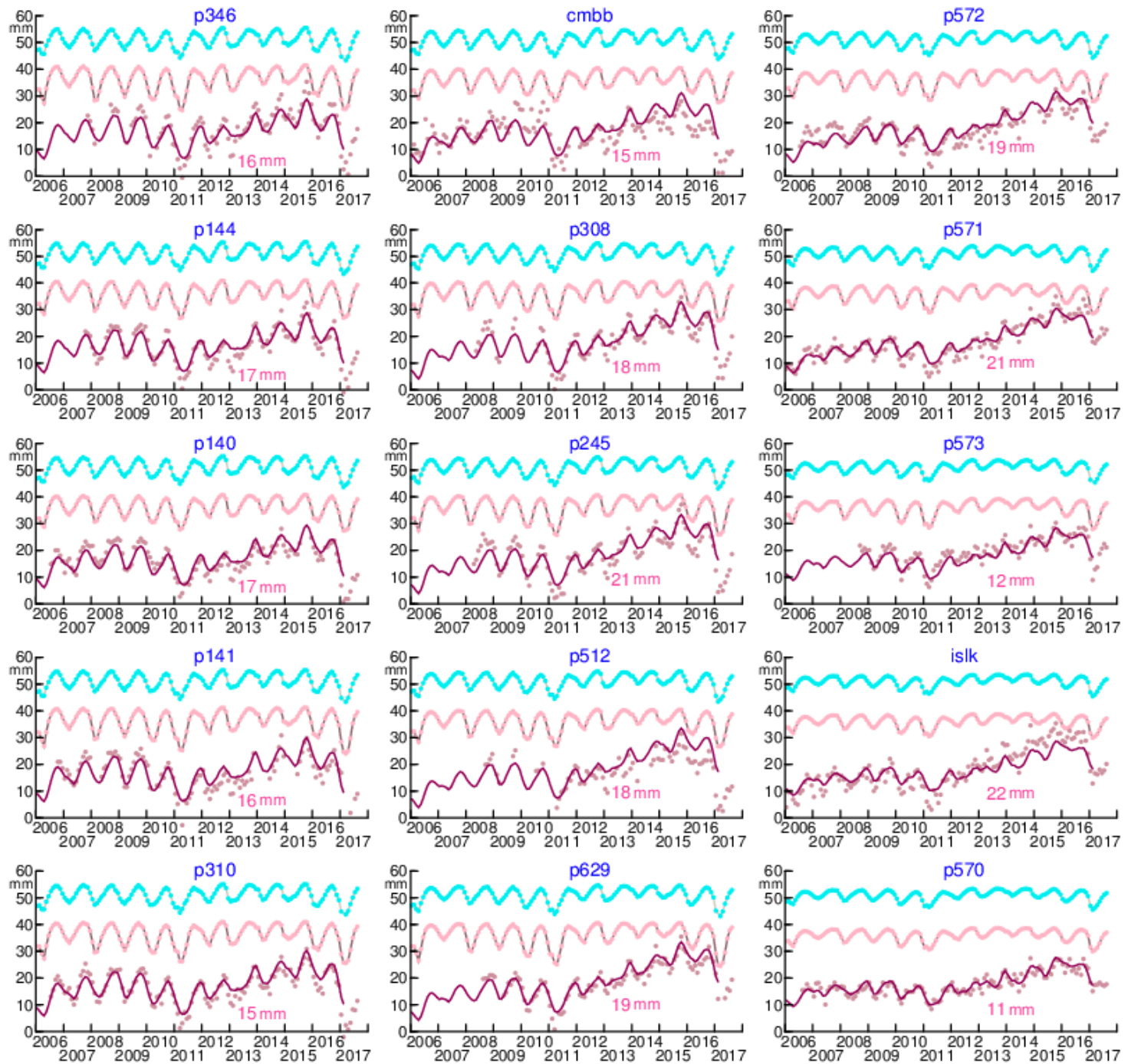
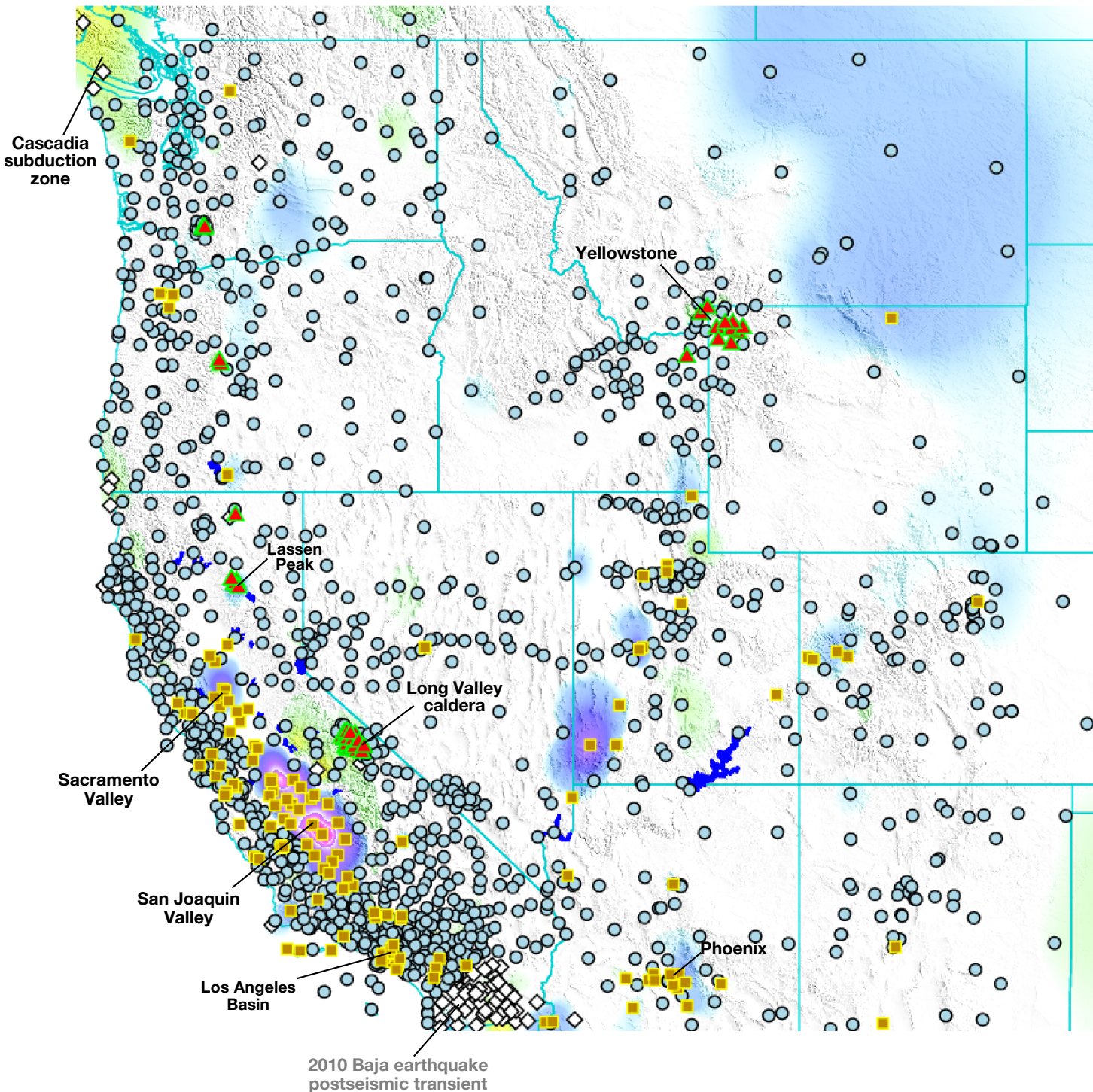


**Fig. S3.** Vertical displacement at GPS sites in the Sierra Nevada. Vertical displacement of 15 GPS sites in the Sierra Nevada after removing elastic deformation produced by known surface water change in artificial reservoirs and estimated groundwater change in the Central Valley (red dots), vertical displacement in hydrology model NLDAS–Noah (blue), and vertical displacement in a composite hydrology model consisting of SNODAS snow water equivalent and NLDAS–Noah soil moisture. The maroon line is vertical displacement calculated from the Unconstrained determination of water change inferred from the GPS vertical displacements corrected for Central Valley groundwater loss (red dots). The GPS sites have nearly zero corrected vertical displacement from 2007 to 2009, subside from 2010 to 2011, and rise from 2012 to 2015. The red numerals give residual uplift from October 2011 to October 2015. SNODAS is the Snow Data Assimilation System [NOHRSC 2004]. NLDAS is the North America Global Assimilation System [Mitchell et al. 2004].

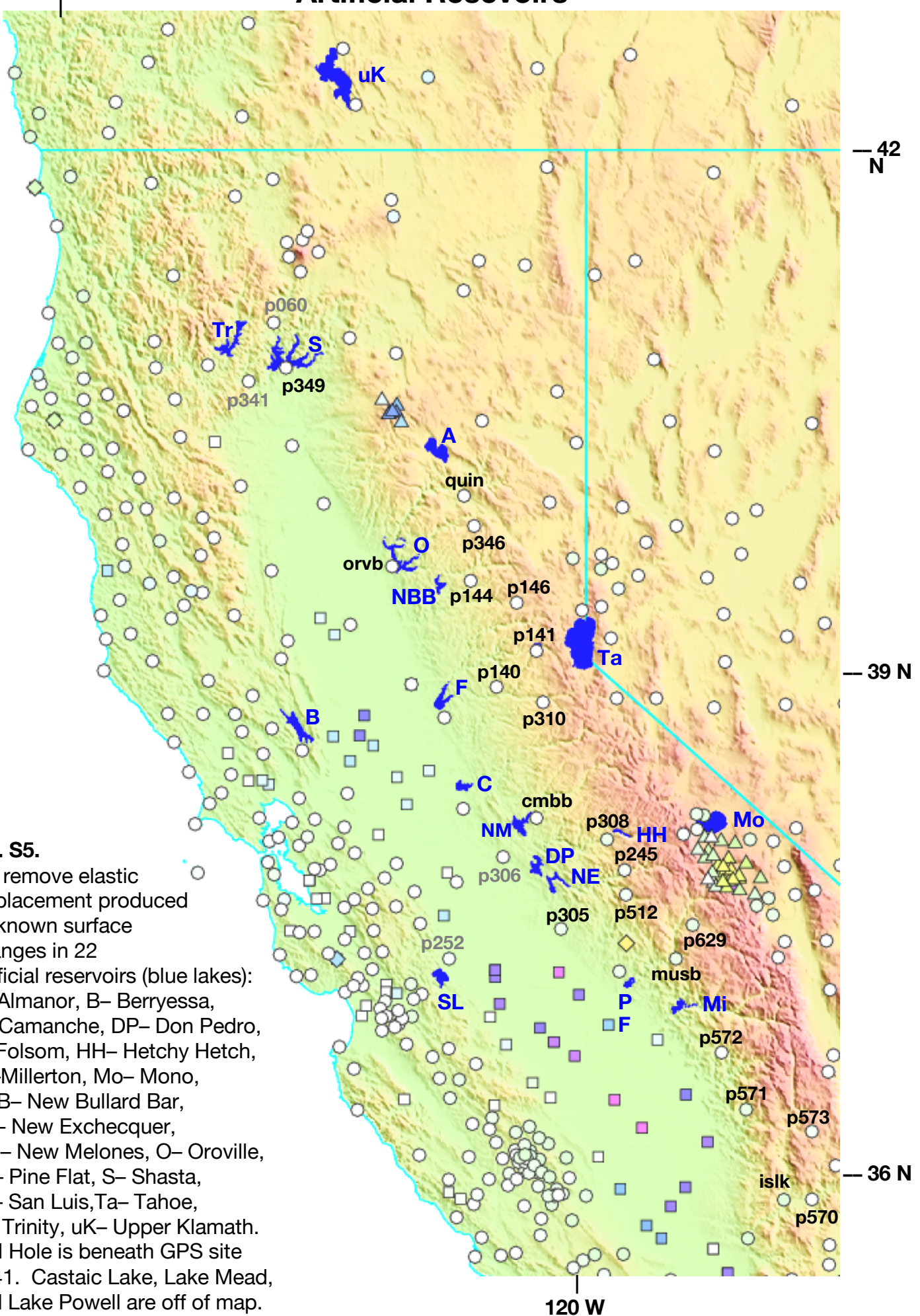
## GPS Sites



Omit	
■	159 Aquifers
▲	57 Volcanoes
◇	84 Baja, Cascadia
Keep	
○	1276 Water elastic

**Fig. S4.** Of a total of 1576 GPS sites, we omit 159 sites recording porous response to groundwater change, 57 sites affected by volcanic activity, and 84 sites influenced by Cascadia subduction, the 2010 Baja Earthquake postseismic transient, and other interfering phenomena. Vertical displacements at the remaining 1276 GPS sites record solid Earth's elastic response to mass loading and are inverted for change in water storage.

# Artificial Reservoirs



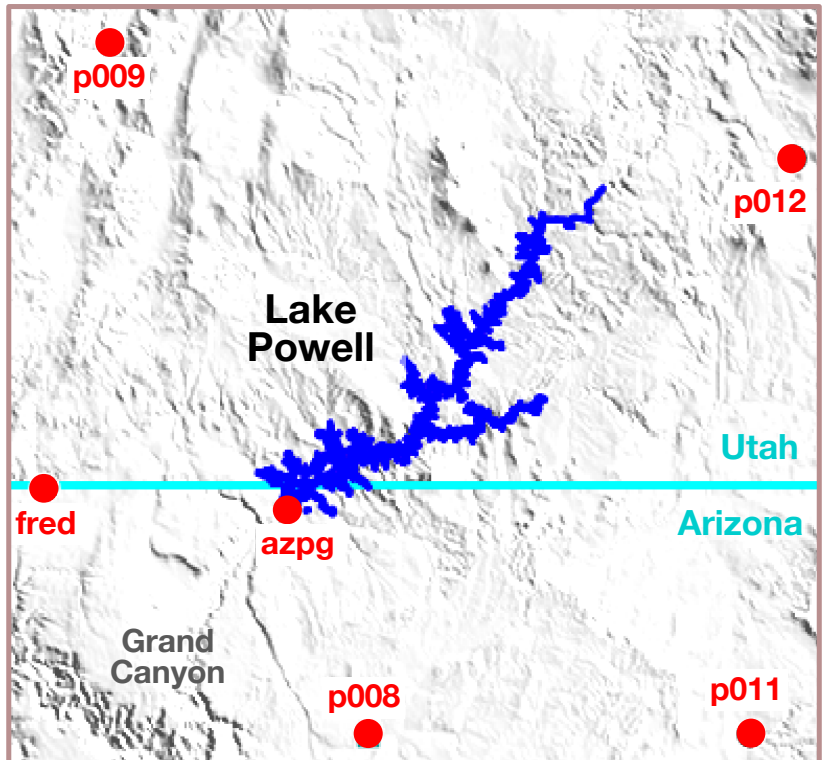
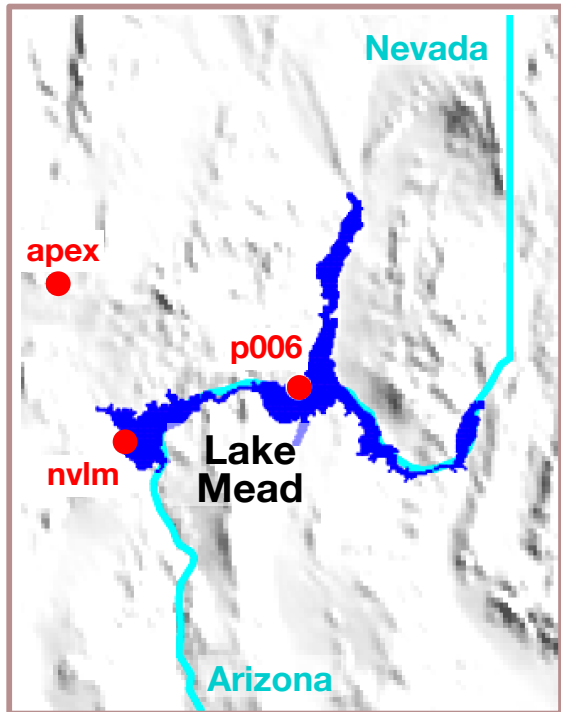


**Fig. S6.** We remove elastic displacement produced by known surface changes at Lake Mead and Lake Powell.

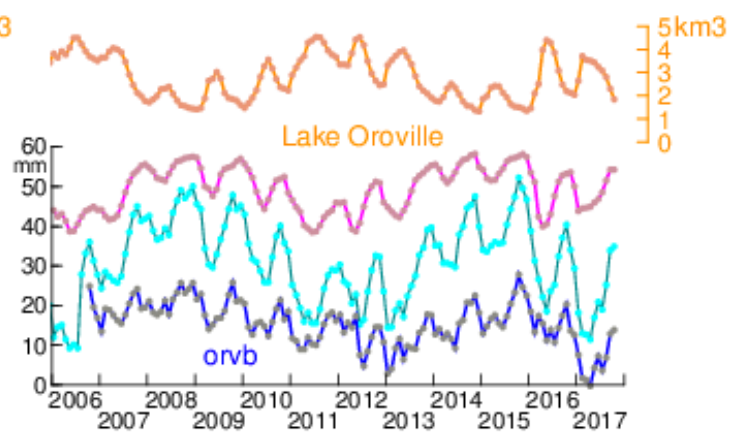
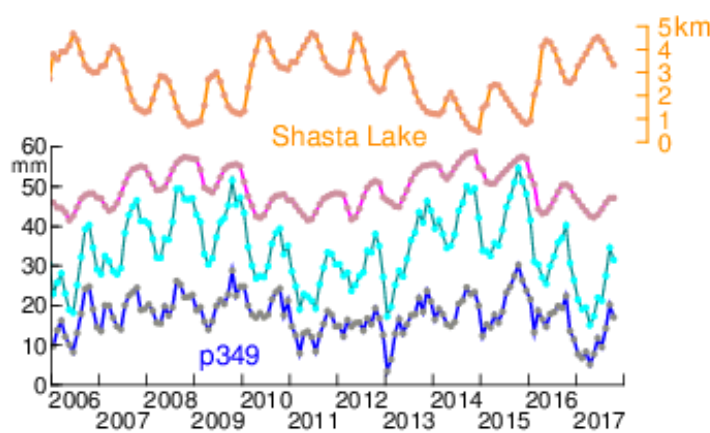
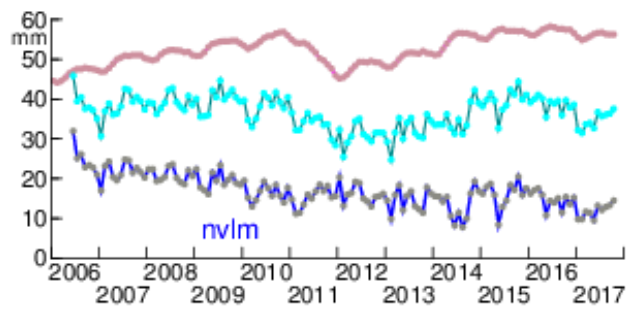
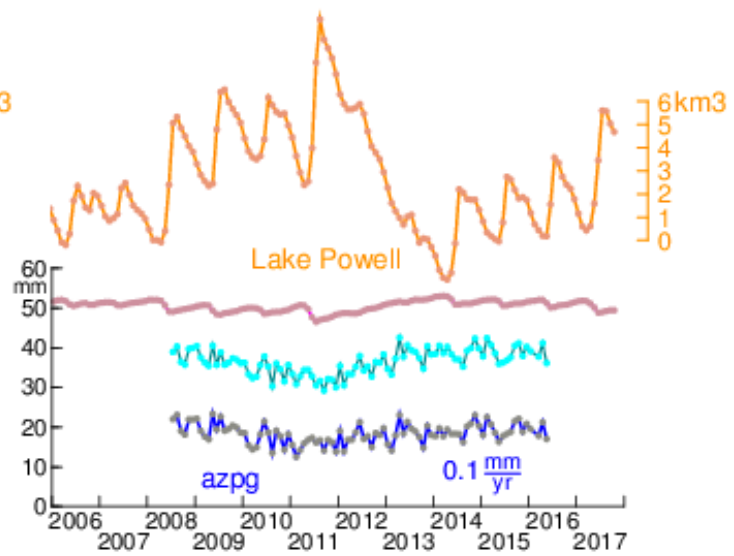
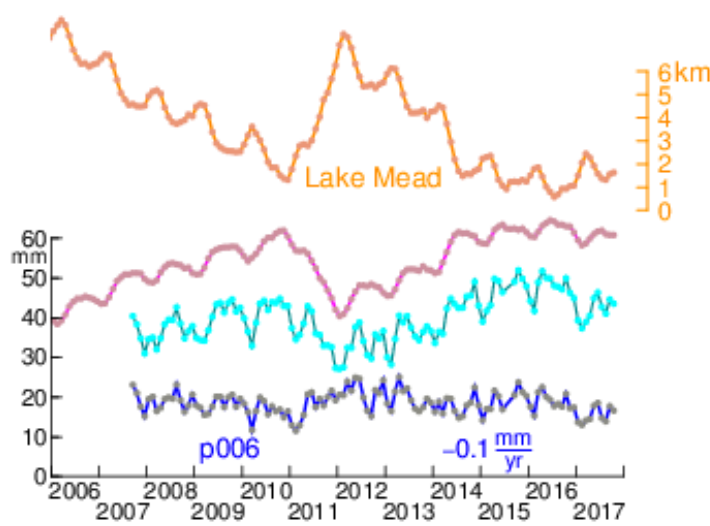


**Fig. S7.** Artificial reservoir surface water changes and vertical displacements at GPS sites. Known changes in surface water in artificial reservoirs (orange) produce elastic vertical displacements (pink). The GPS observations (light blue) are corrected for this elastic deformation, resulting in smaller residual vertical displacement (blue-gray). The residual mean vertical rate is given for p006 and apzg.

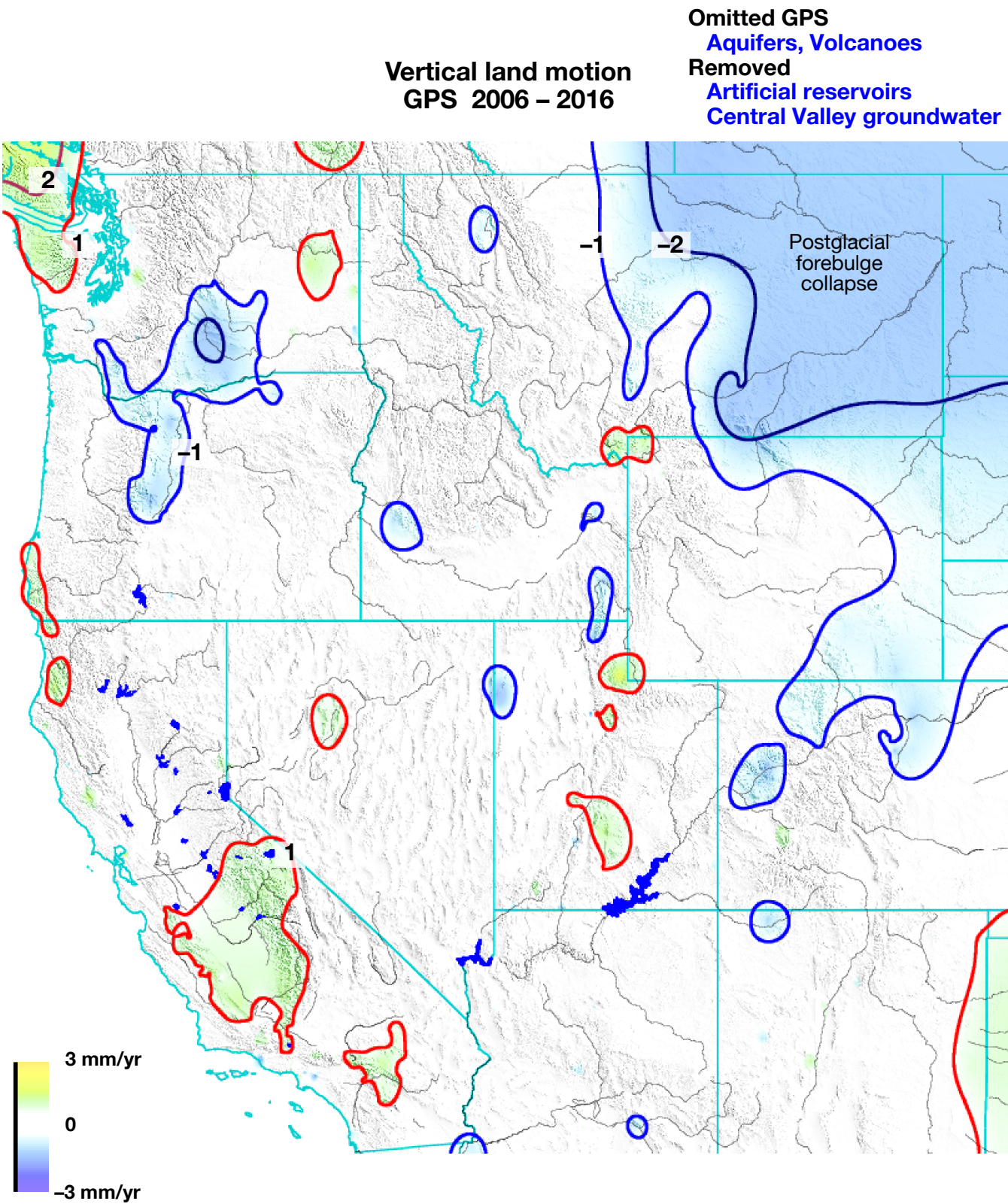


**Fig. S8.** Vertical land motion recording solid Earth's elastic response to mass change. The vertical surface is fit to 1276 GPS vertical rates after omitting sites on top of aquifers and near volcanoes and after removing elastic displacement produced by known surface water changes in artificial reservoirs and by estimated groundwater changes in the Central Valley. Contours are at  $-2 \text{ mm/yr}$ ,  $-1 \text{ mm/yr}$ ,  $1 \text{ mm/yr}$ , and  $2 \text{ mm/yr}$ . Nearly all of the western U.S. has a mean rate of vertical motion less than  $2 \text{ mm/yr}$ . We invert the vertical displacements at these 1276 GPS sites to infer changes in water storage.

## Postglacial rebound ICE-6G\_C (VM5a)

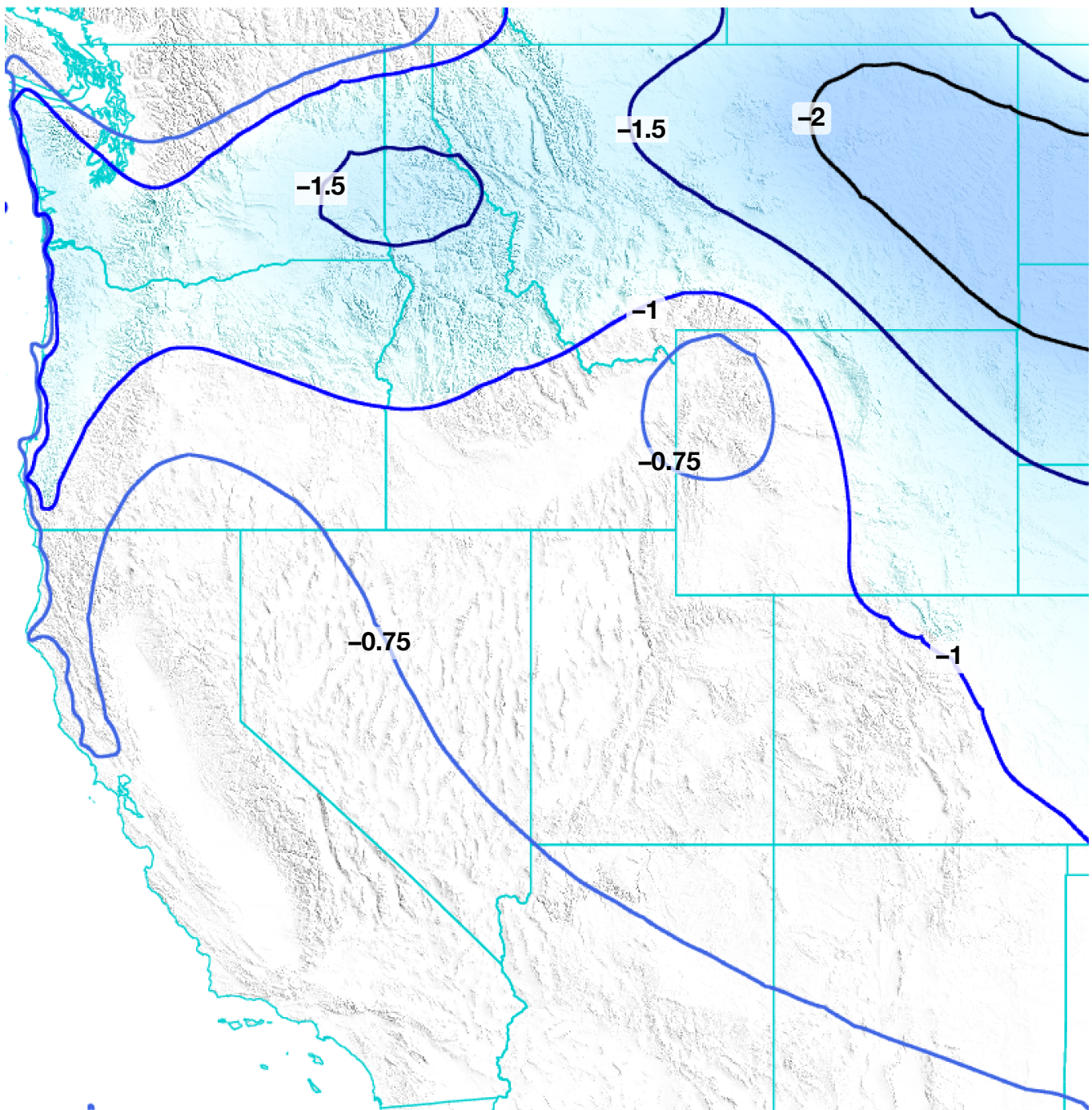


**Fig. S9.** Vertical land motion predicted by postglacial rebound model ICE-6G (VM5a) [Peltier et al. 2015, Argus et al. 2014b]

## Vertical land motion GPS 2006 – 2016

Omitted GPS  
Aquifers, Volcanoes  
Removed  
Artificial reservoirs  
Postglacial rebound

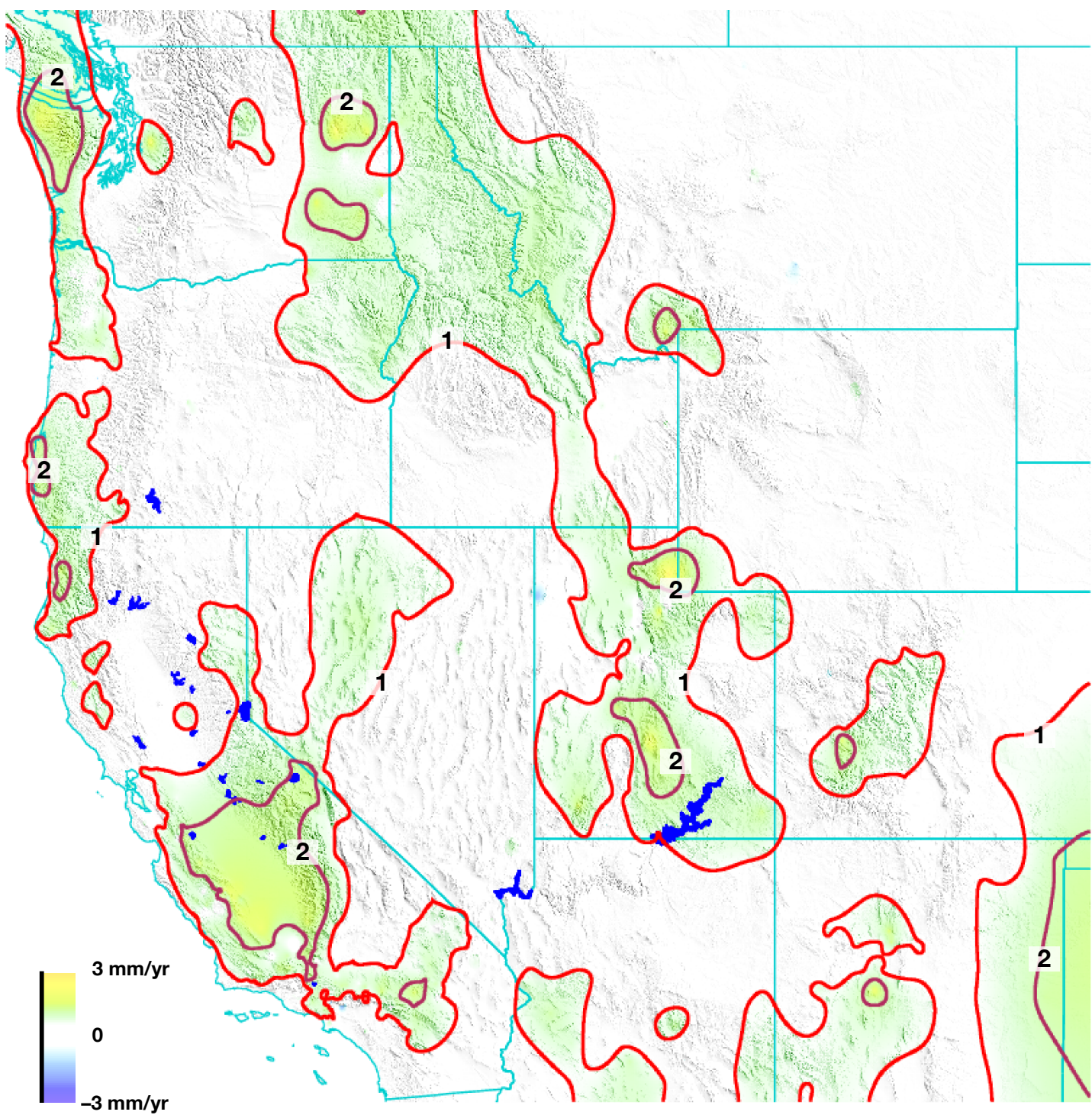


**Fig. S10.** Vertical land motion recording solid Earth's elastic response to mass change after removing postglacial rebound. The postglacial rebound predictions of model ICE-6G\_C (VM5a) Peltier et al. 2015, Argus et al. 2014] are removed from the vertical motions in Fig. S4a.

## Vertical land motion GPS 2006 – 2016

Omitted GPS  
 Aquifers, Volcanoes  
 Removed  
 Artificial reservoirs  
 Postglacial rebound  
**CM**  
 Minimize vertical

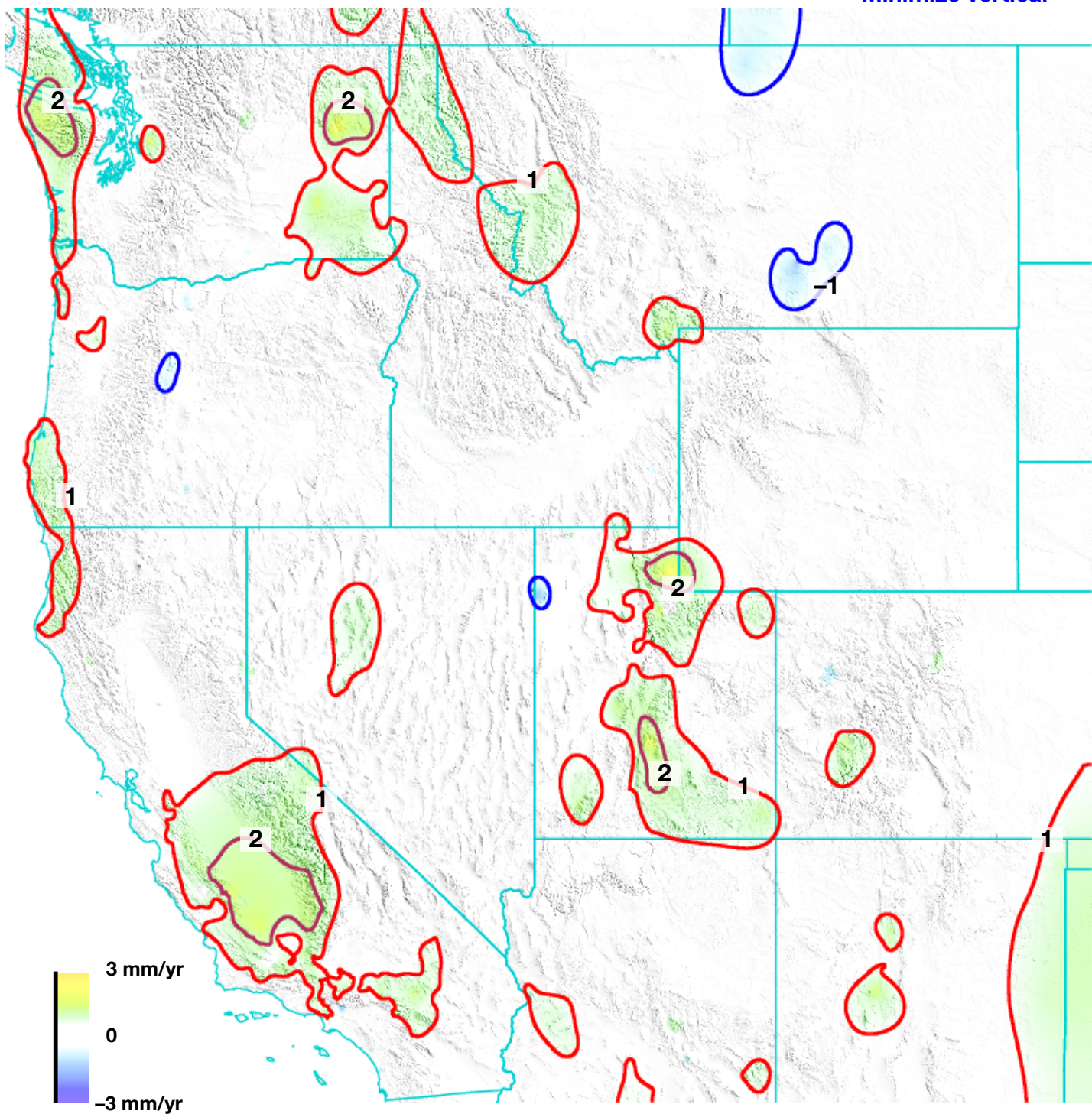


**Fig. S11.** Vertical land motion recording solid Earth's elastic response to mass change after removing postglacial rebound and adjusting the velocity of CM. The postglacial rebound predictions of model ICE-6G\_C (VM5a) Peltier et al. 2015, Argus et al. 2014] are removed from the vertical motions in Fig. S4, and the velocity of CM is adjusted relative to ITRF 2008 [Altamimi et al. 2011] by X 0.2, Y -0.1, and Z 0.6 mm/yr [Argus et al. 2014].

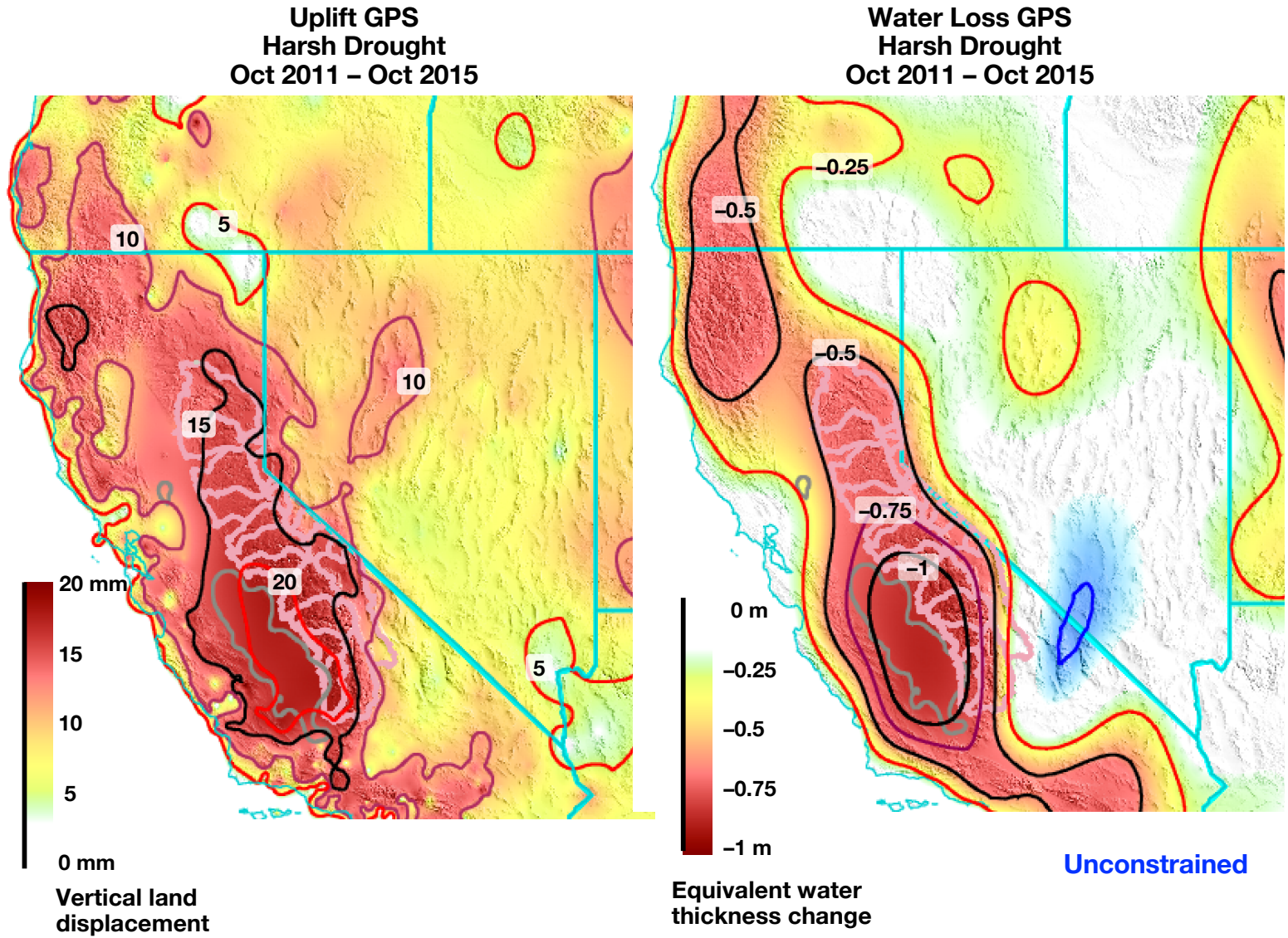
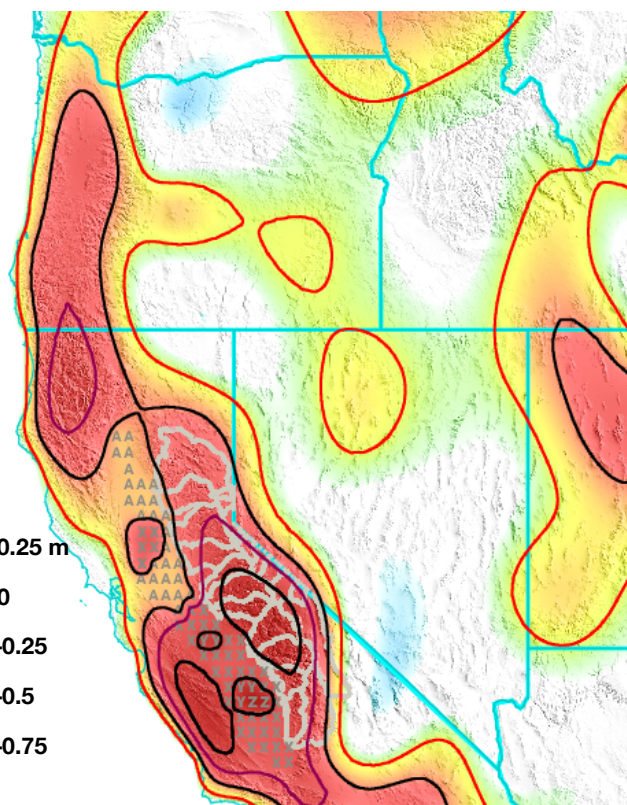
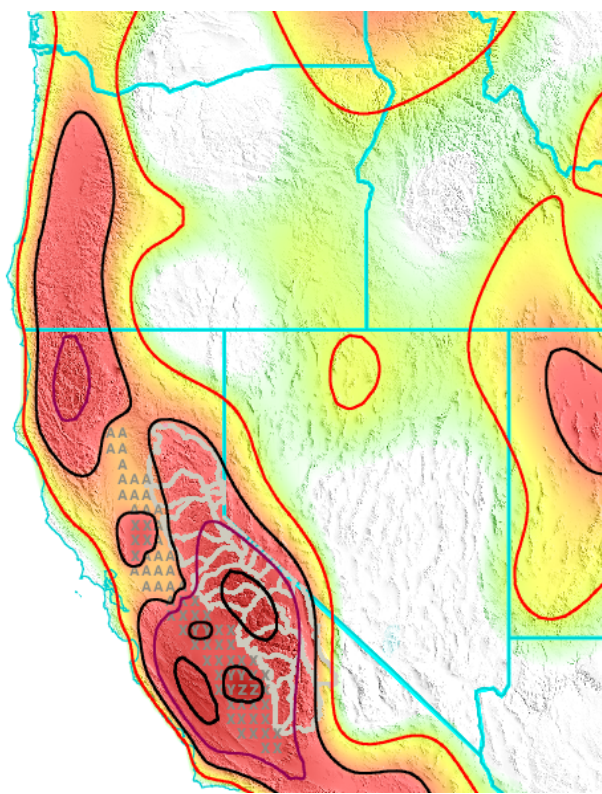


**Fig. S12.** Vertical land displacement from GPS (left) and change in total water storage (right) during severe drought from October 2011 to October 2015 in the Unconstrained model. Elastic vertical displacement produced by unloading of the a priori model in Fig. 2b has been removed. Water loss in the Sierra Nevada from October 2011 to October 2015 is just  $4 \text{ km}^3$  smaller in this Unconstrained model than in the Constrained model in Fig. 7. However, water loss in the Central Valley from October 2011 to October 2015 is twice as large in this Unconstrained model ( $-76 \text{ km}^3$ , after adding back in the  $-34 \text{ km}^3$  of groundwater loss implicitly removed from the GPS data) as in the Constrained model ( $-34 \text{ km}^3$ ).

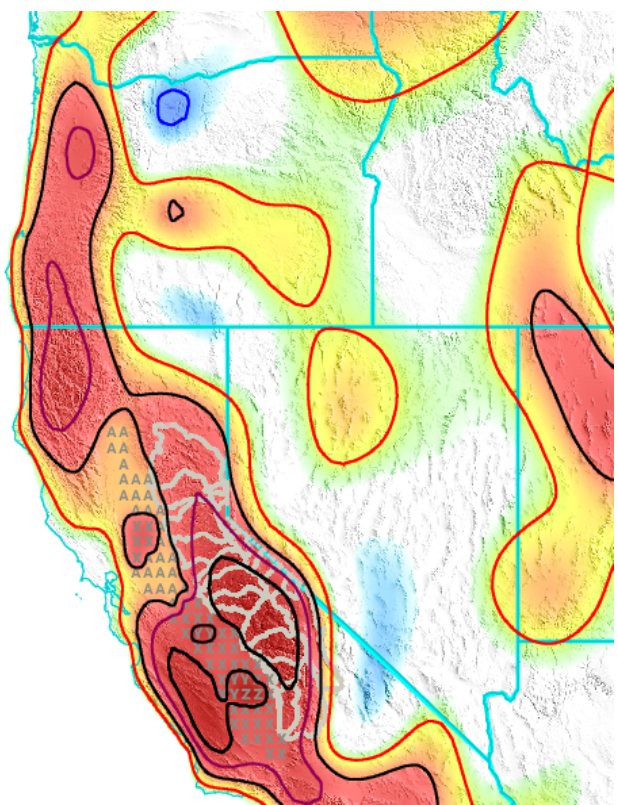
**Water Loss GPS  
Harsh Drought  
Oct 2011 – Oct 2015**



**Optimal smoothing**  
 $\sigma_2$  18 mm  
rms 3.8 mm misfit  
Sierra Nevada  $-45 \pm 21 \text{ km}^3$



**Strong smoothing**  
 $\sigma_2$  12 mm  
rms 4.0 mm misfit  
Sierra Nevada  $-42 \text{ km}^3$

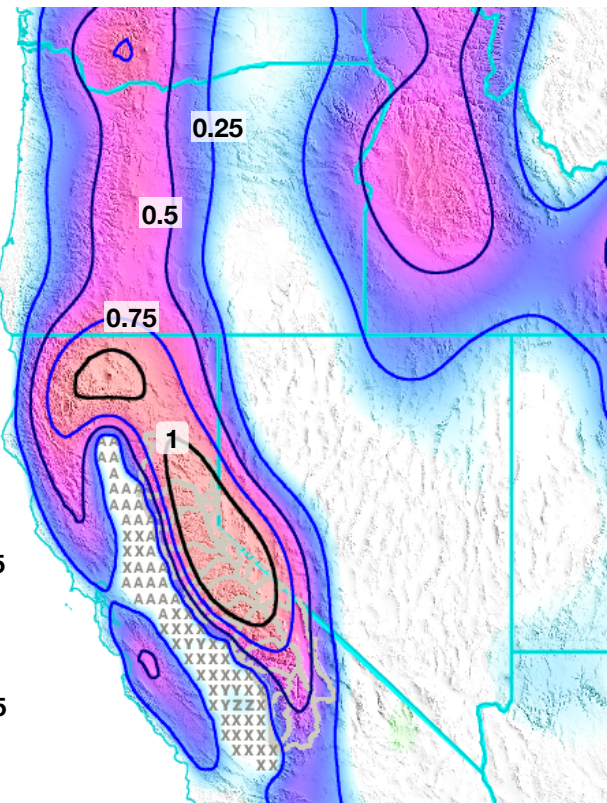
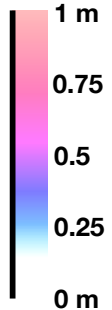


**Weak smoothing**  
 $\sigma_2$  27 mm  
rms 3.7 mm misfit  
Sierra Nevada  $-48 \text{ km}^3$

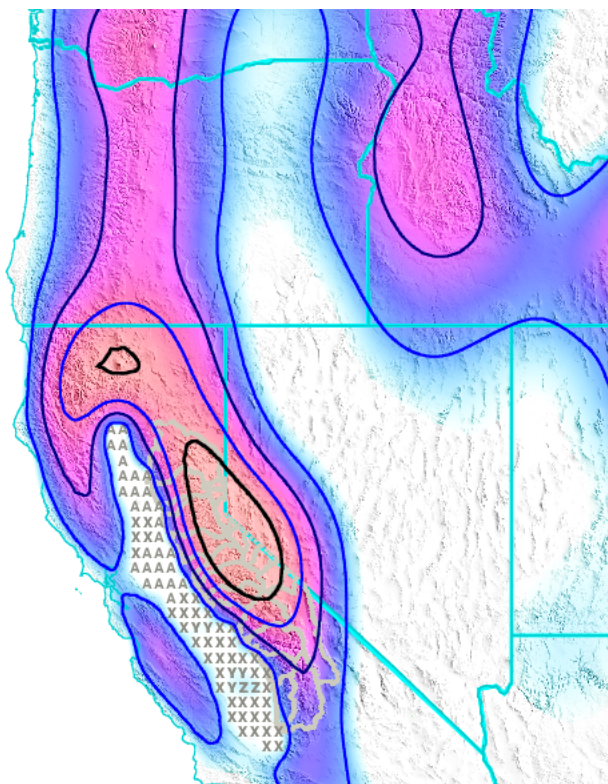
**Fig. S13.**

Water Gain GPS  
Strong Rainy Season  
Oct 2016 – Apr 2017

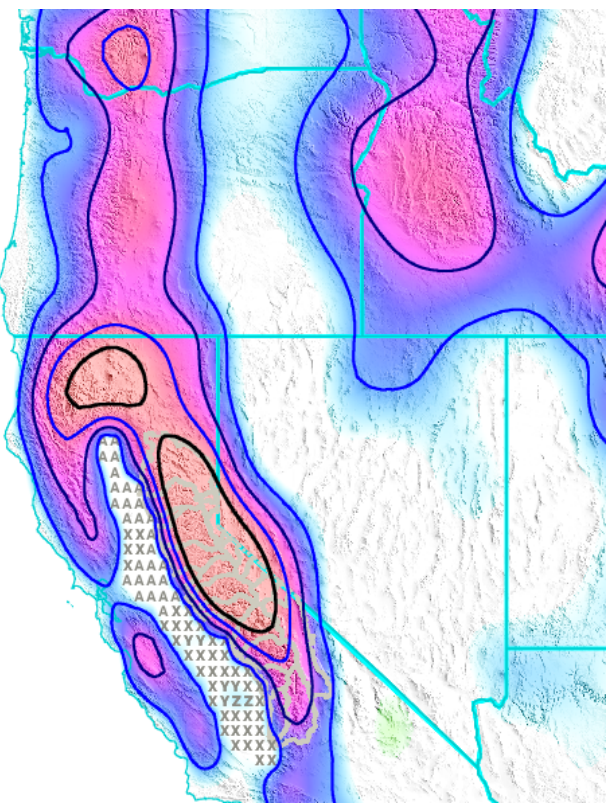
Equivalent water thickness change



Optimal smoothing  
 $\sigma_2$  18 mm  
rms 2.6 mm misfit  
Sierra Nevada  
 $45 \pm 15 \text{ km}^3$



Stronger smoothing  
 $\sigma_2$  12 mm  
rms 2.7 mm misfit  
Sierra Nevada  
 $39 \text{ km}^3$



Weaker smoothing  
 $\sigma_2$  27 mm  
rms 2.6 mm misfit  
Sierra Nevada  
 $51 \text{ km}^3$

Fig. S14.

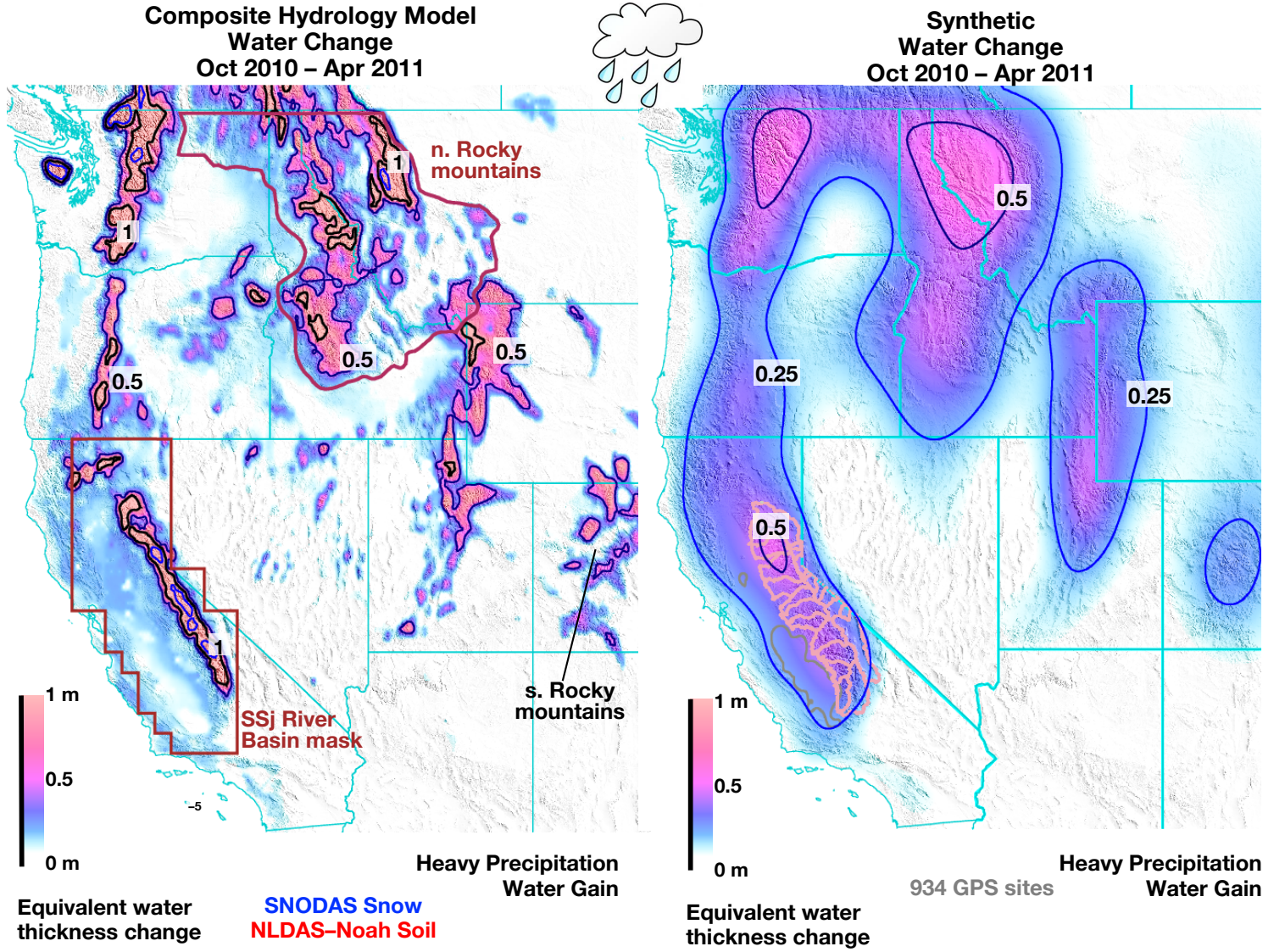


**Fig. S15.**

(Left) Change in water storage in a composite hydrology model during heavy precipitation from Oct 2010 to Apr 2011. This composite hydrology model consists of snow water equivalent in SNODAS and soil moisture in NLDAS-Noah. Water Years 2011 and 2017 were the years with the most precipitation in the past 11 years. Change in water storage in the Sacramento-San Joaquin (SSj) River basin mask of Wiese et al. [2016] and the northern Rocky mountains province (maroon outline) are plotted in Fig. S13.

(Right) Change in water storage determined in an inversion of synthetic data generated on the basis of the composite hydrology model at left. The recovered changes in total water storage are smoothed in space slightly relative to the tight clustering of snow in the hydrology model

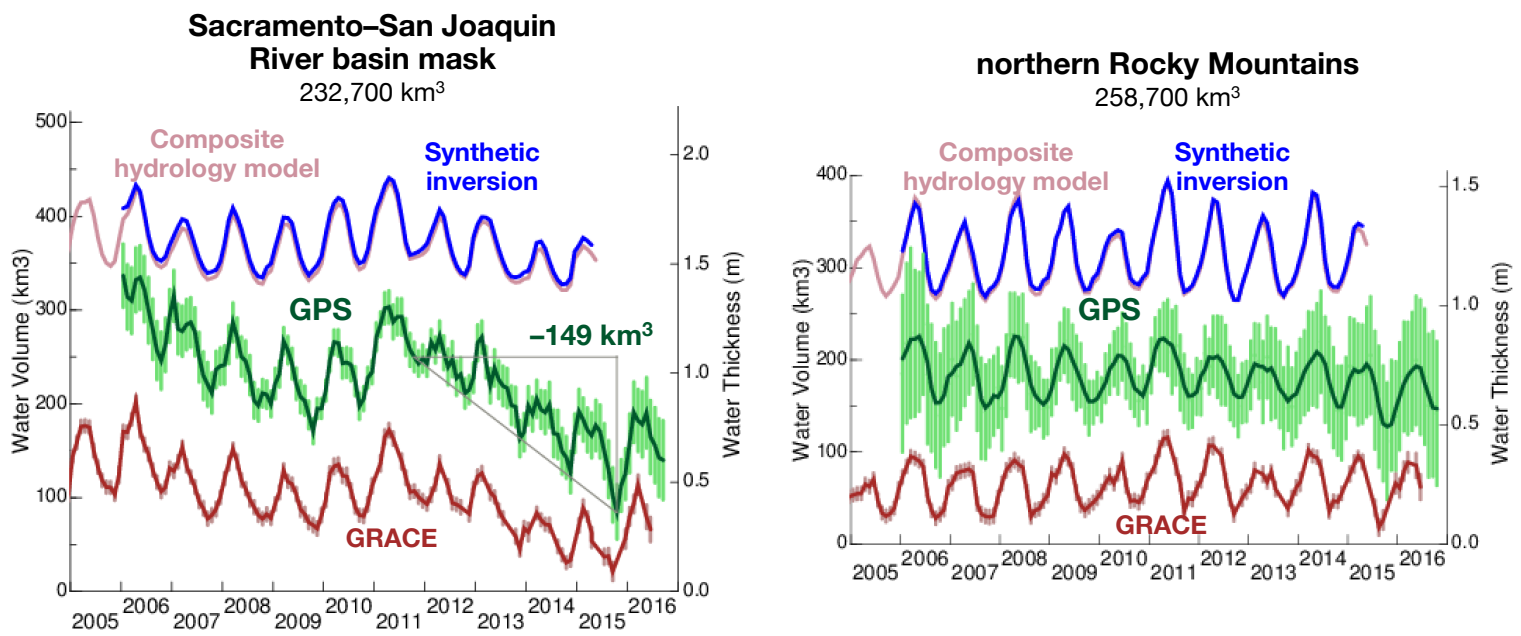


**Fig. S16.** Change in total water storage is compared between the composite hydrology model and the inversion of synthetic GPS vertical displacements calculated from the hydrology model for the Sacramento–San Joaquin River basin mask and the northern Rocky Mountains (see Fig. S12). Water change inferred from GPS and determined from GRACE is also plotted.

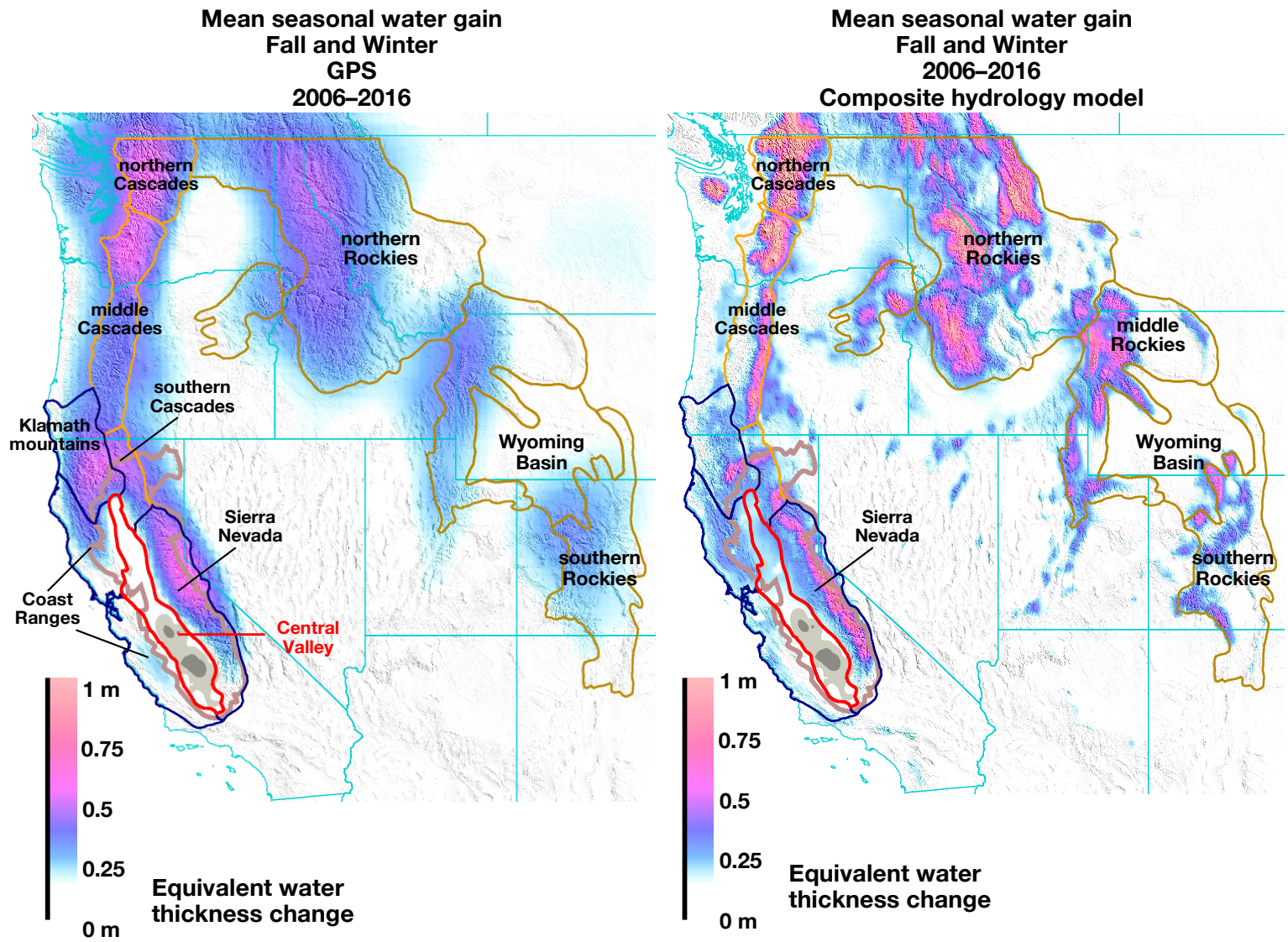


**Fig. S17.** Mean seasonal water gain in the fall and winter inferred from GPS in this study (left) and in a composite hydrology model (right). This mean increase in equivalent water thickness from Oct 1 to Apr 1 is calculated from the sinusoid fit to change in total water storage inferred from GPS or in the hydrology model from Jan 2006 to Dec 2016. Physiographic provinces are from Thelin and Pike [1991]. See Fig. 1 for names of provinces in California.

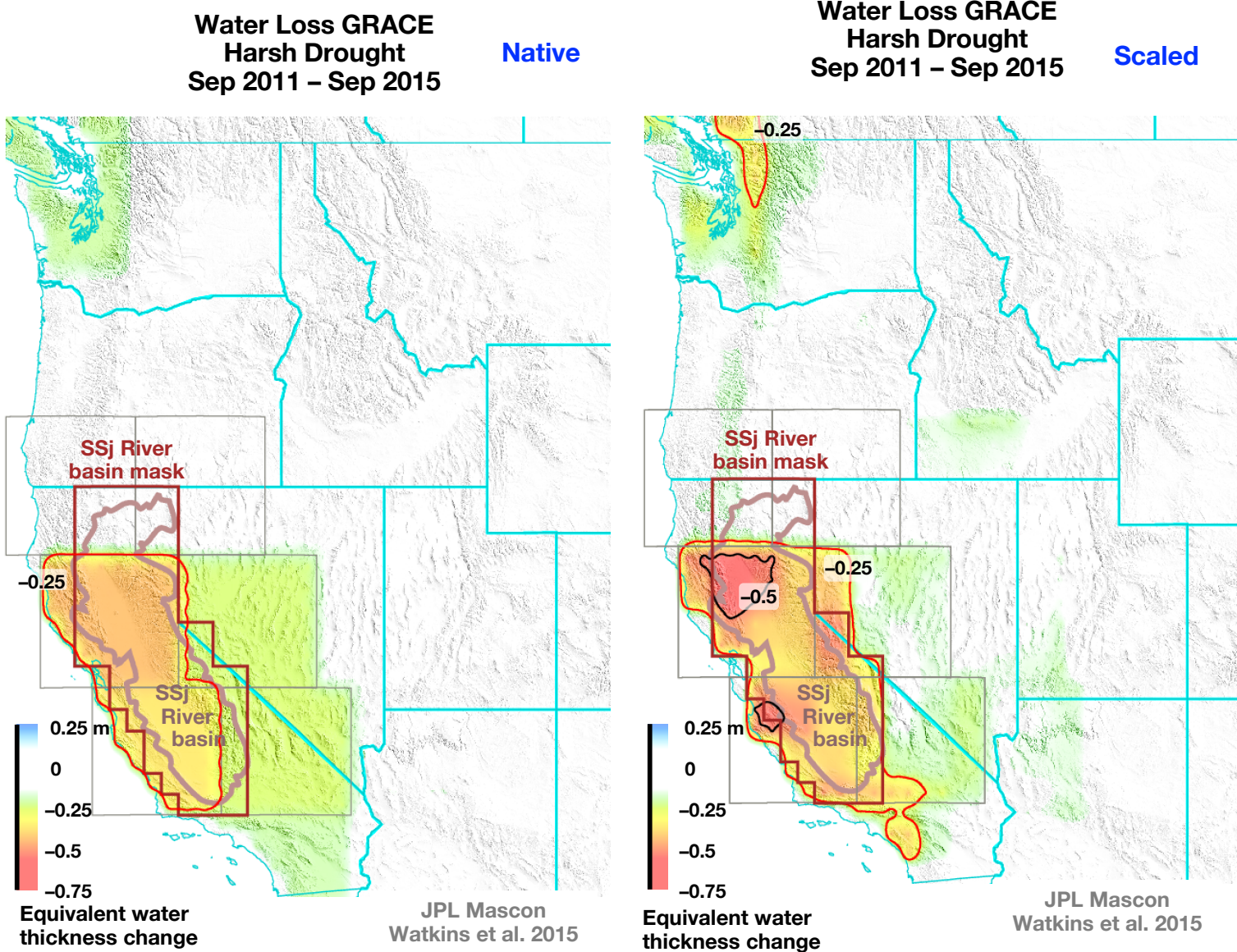


**Fig. S18.** Water loss during severe drought from Sep 2011 to Sep 2015 inferred from GRACE at (left) native 330 km spatial resolution and (right) corrected for leaking using scaling factors based on seasonal water oscillations in the Climate Land Model [Lawrence et al. 2011]. Water change in the native GRACE solution adheres to 3° mascons (6 light gray squares). The Sacramento-San Joaquin River basin mask (maroon outline) of Wiese et al. [2016] is 50 per cent bigger than the true River basin (light brown outline).

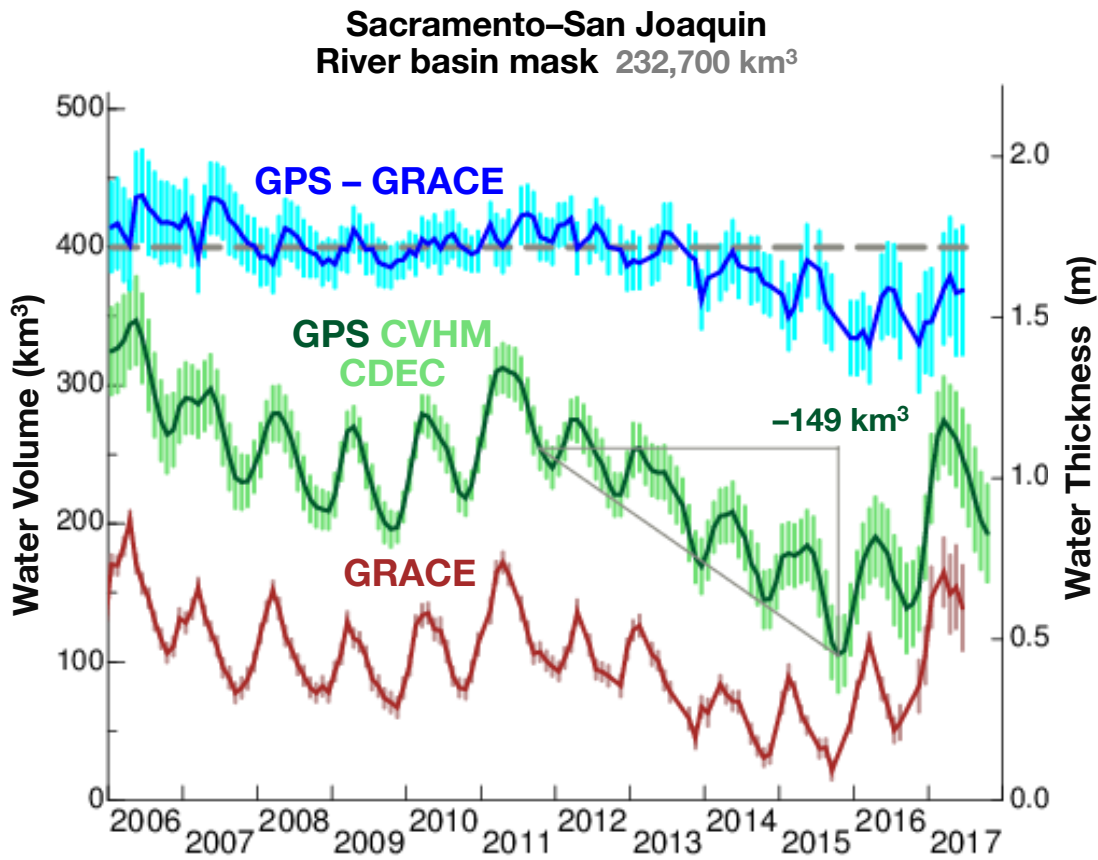


**Fig. S19** Change in total water storage in the Sacramento–San Joaquin River basin mask of Wiese et al. [2016], which is 50% larger in area than the true River basin (in Fig. 1.) Leakage of mass change inferred for this larger mask is believed to be less than for the true River basin. Water gain in the bigger River basin mask from October 2009 to October 2011 is inferred from GPS, CVHM, and CDEC to be  $59 \pm 29 \text{ km}^3$ , a factor of 1.6 times greater than the  $37 \pm 14 \text{ km}^3$  estimated from GRACE (95% confidence limits). Water loss in the larger River basin mask from October 2011 to October 2015 is inferred from GPS, CVHM, and CDEC to be  $149 \pm 53 \text{ km}^3$ , nearly twice the  $85 \pm 19 \text{ km}^3$  inferred from GRACE. The difference between the GPS and GRACE estimates is  $22 \pm 32 \text{ km}^3$  for October 2009 to October 2011 and  $64 \pm 55 \text{ km}^3$  for October 2011 to October 2015.

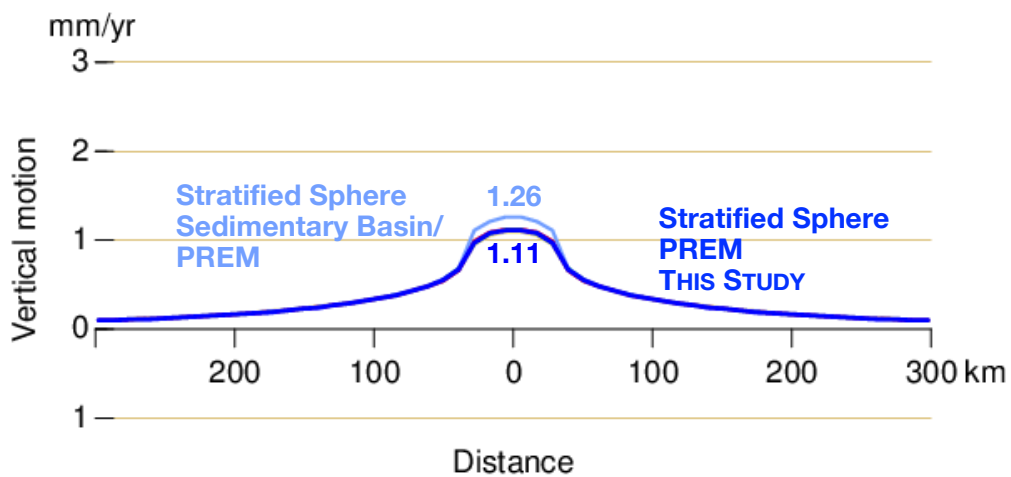
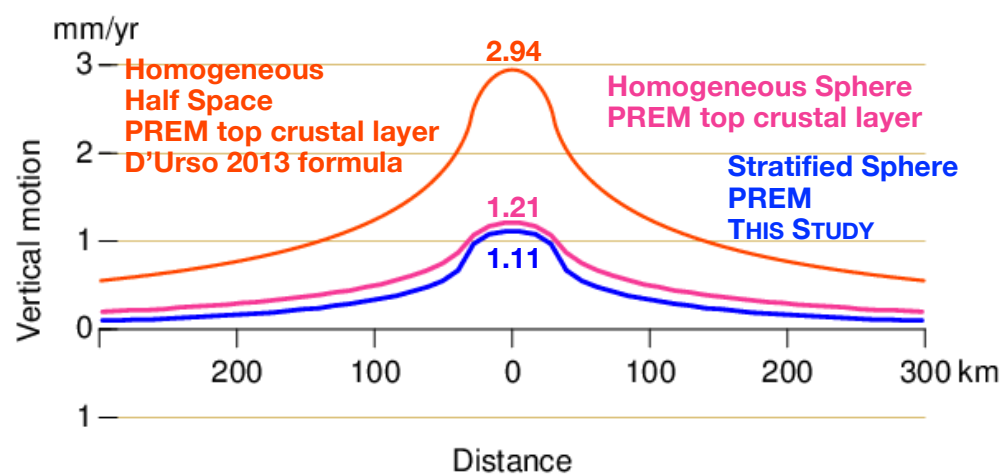
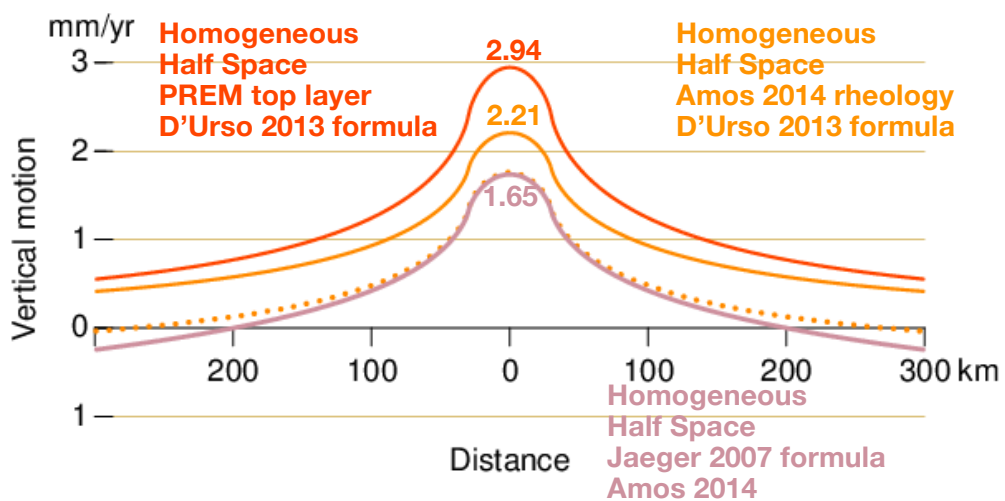


**Fig. S20.** The caption is on the next page.

**Fig. S20.** Models of solid Earth's elastic response to unloading of Central Valley groundwater at  $-4 \text{ km}^3/\text{yr}$  distributed evenly across a  $450 \text{ km} \times 60 \text{ km}$  region. This illustration presents intermediate models between the homogeneous, half space determination of Amos et al. [2014] and the stratified, gravitating, spherical determination in This Study (see Fig. 11).

**(Top)** The homogeneous, half space model calculated by Amos et al. [2014] using the rock mechanic formula of Jaeger et al. [2007] is compared to the homogeneous, half space model calculated using the formula of D'Urso and Marmo [2013] for the Amos 2014 rheology and for the rheology in the top PREM layer. The D'Urso, Marmo 2013 /Amos rheology and Amos 2014 calculations have a similar decrease in vertical displacement going away from the center of the load but the D'Urso, Marmo 2013 calculation is offset in the vertical from the Amos 2014 calculation upward by  $0.56 \text{ mm/yr}$ . The D'Urso, Marmo 2013 /PREM rheology calculation has 33% more uplift than the D'Urso, Marmo 2013/Amos rheology because the top layer of PREM (Young's modulus  $E$   $66.5 \text{ GPa}$ ) is softer than the Amos 2014 rheology ( $E$   $87.5 \text{ GPa}$ ).

**(Middle)** The homogeneous, half space model calculated using the D'Urso, Marmo 2013 formula for the top layer of PREM is compared to a homogeneous, gravitating, spherical model from Green's functions also for the top layer of PREM calculated by H. R. Martens, and to This Study's stratified, gravitating, spherical model from Green's functions for full PREM [Wang et al. 2012]. Going from a homogeneous half space to a homogeneous, gravitating sphere reduces uplift at the load center by a factor of 2.5. Going from a homogenous sphere to a stratified sphere reduces uplift by 10% at the load center and by 25% at a distance of 50 km from the load center.

**(Bottom)** A stratified gravitating, spherical model from Green's functions that we calculated for the Los Angeles sedimentary basin (CVM-H v.15.1.0 [Shaw et al. 2017]) in the top 34 km and PREM beneath 34 km is compared to This Study's stratified, gravitating, spherical model for full PREM [Wang et al. 2012]. PREM and the CVM-H have similar rheology from 5 km to 34 km depth; the sedimentary basin in the top 5 km in CVM-H is the primary cause of the difference between the two models. Incorporating the sedimentary basin increases uplift at the load center by 14%. Also plotted but indistinguishable from This Study's stratified, gravitating, spherical model for full PREM is a stratified, spherical model for the San Joaquin Valley in the top 20 km and PREM beneath 20 km.